VIP Hydrogen-Evolution Catalysts Very Important Paper
Deutsche Ausgabe: DOI: 10.1002/ange.201504985
Internationale Ausgabe: DOI: 10.1002/anie.201504985

A Graphitic-C_3N_4 "Seaweed" Architecture for Enhanced Hydrogen Evolution**

*Qing Han, Bing Wang, Yang Zhao, Chuangang Hu, and Liangti Qu**

Abstract: *A seaweed-like graphitic-C_3N_4 (g-C_3N_4 "seaweed") architecture has been prepared by direct calcination of the freeze-drying-assembled, hydrothermally treated dicyandiamide fiber network. The seaweed network of mesoporous g-C_3N_4 nanofibers is favorable for light harvesting, charge separation and utilization of active sites, and has highly efficient photocatalytic behavior for water splitting. It exhibits a high hydrogen-evolution rate of 9900 $\mu mol\,h^{-1}\,g^{-1}$ (thirty times higher than that of its g-C_3N_4 bulk counterpart), and a remarkable apparent quantum efficiency of 7.8 % at 420 nm, better than most of the g-C_3N_4 nanostructures reported. This work presents a very simple method for designing and developing high-performance catalysts for hydrogen evolution.*

Energy deficiency and environmental pollution are an urgent problem all over the world. Clean hydrogen energy is one of the most promising replacement energy resources owing to its environmental benignity and recyclability. Photochemical water splitting to generate hydrogen by utilizing a photocatalyst, only consuming solar energy, has become the main trend for hydrogen-energy production. Hence, the research and development of new highly effective photocatalysts that can make full use of solar energy by transforming it to hydrogen energy has been a research focus in photocatalysis field.[1,2]

Graphitic carbon nitride (g-C_3N_4) which has suitable conduction-band and valence-band levels for generating hydrogen and oxygen has attracted considerable interest.[3] It has been considered one of the most promising photocatalysts for hydrogen production owing to its good chemical stability, anti-photocorrosion, visible-light response, and easily adjustable electronic-band structure. Unfortunately, the catalytic activity of pristine g-C_3N_4 for hydrogen evolution is quite low. In this regard, various strategies have been proposed to improve the performance including the doping with metal/non-metal, creation of heterojunctions, composition, and formation of nanoarchitectures.[4] Among them, nanostructuring g-C_3N_4 with controllable morphologies is an efficient way to enhance the photocatalytic activity. To date, the nanostructured g-C_3N_4 including nanobelts,[5] nanosheets,[6] and nanospheres[7] have emerged, but the assembly of low-dimensional g-C_3N_4 nanostructures into macroscopic architectures for hydrogen evolution is rarely reported probably because of the rigorous reaction conditions and complicated preparation process and associated high cost.[8a]

Generally, there are two approaches to manufacture nanostructured g-C_3N_4. One way is with the aid of organic reagents[5,8] or catalysts[9] to form a desired size and shape. However, this type of method often involves tedious purification procedures to separate the desirable nanoparticles from complex reactant mixtures. An alternative is to use silica as a template, however this approach inevitably requires the removal of the template by environmentally hazardous reagents.[10] As a result, a simple, environmentally friendly and low-cost method for large-scale production of nanostructured g-C_3N_4 photocatalysts with dramatically enhanced photocatalytic activity is needed.

Herein, we present a straightforward, but effective template-free methodology for the large-scale production of g-C_3N_4 "seaweed" which consists of porous fiber structures. Dicyandiamide was used as the starting material undergoing the hydrothermal treatment and vacuum freeze-drying technology was exploited to activate the self-assembly for the formation of the macroscopic network of fiber-like structures. Subsequently, the calcination of the precursor generated the network architectures of g-C_3N_4 "seaweed" which is rich in mesopores. The g-C_3N_4 "seaweed" exhibits a very high rate of hydrogen production, as high as 9900 $\mu mol\,h^{-1}\,g^{-1}$ under $\lambda >$ 420 nm irradiation, which leads to a high turnover number of 385 after 6 h and results in an outstanding quantum efficiency of 7.8 % at 420 nm.

The pristine dicyandiamide has a square crystal grain size of approximately 1.5 mm (Figure S1 a,b in the Supporting Information) and its morphology was dramatically altered to a white macroscopic monolith consisted of interconnected network of fiber-like structures (Figure 1 a,b) after freeze-drying the hydrothermally treated dicyandiamide (HTD) solution. As shown in Figure 1 c,d, the assembled sample shows drastically reduced grain size compared to pristine dicyandiamide. Typically, a large piece of g-C_3N_4 was obtained by calcining the freeze-drying-assembled HTD at 550 °C (Figure 1 e), which was composed of interlocking fibers of hundreds of nanometers in width and tens of microns in length resembling "seaweed" (Figure 1 f,g) and designated as g-C_3N_4(550) "seaweed". The TEM image revealed that the microfibers were enriched with mesopores of less than 20 nm (Figure 1 h and its inset). Compared to g-C_3N_4 bulk (Figure S2 a,b), g-C_3N_4(550) "seaweed" features a morphology of

[*] Q. Han, B. Wang, Y. Zhao, C. Hu, Prof. L. Qu
Beijing Key Laboratory of Photoelectronic/Electrophotonic Conversion Materials, Key Laboratory of Cluster Science, Ministry of Education, School of Chemistry, Beijing Institute of Technology
Beijng 100081 (P.R. China)
E-mail: lqu@bit.edu.cn

[**] We thank the financial support from the 973 program of China (2011CB013000) and NSFC (21325415, 21174019), Beijing Natural Science Foundation (2152028) and 111 Project 807012.

Supporting information for this article is available on the WWW under http://dx.doi.org/10.1002/anie.201504985.

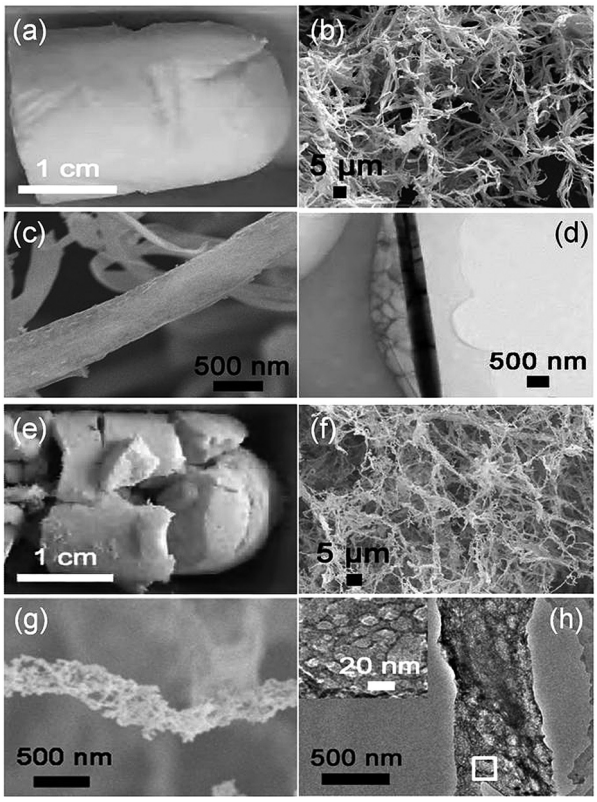

Figure 1. a) Photograph and b) low-, c) high-magnification SEM images of the freeze-dried, hydrothermally treated dicyandiamide (HTD); d) TEM image of a single fiber of the freeze-dried HTD; e) Photograph and f) low-, h) high-magnification SEM images of g-C_3N_4 (550) "seaweed"; h) TEM image of a fiber of g-C_3N_4 (550) "seaweed" (Inset: the enlarged view of the rectangle area).

thin and porous fibers (detailed discussion in Supporting Information). Nitrogen adsorption–desorption isotherms (Figure 2a) show that the nitrogen uptake of g-C_3N_4 (550) "seaweed" is significantly greater in the high-pressure range than for g-C_3N_4 bulk, indicating the existence of mesopores. The Brunauer–Emmett–Teller (BET) surface area of g-C_3N_4 (550) "seaweed" is approximately 130 $m^2 g^{-1}$, which is over 10-times higher than that of g-C_3N_4 bulk (ca. 12 $m^2 g^{-1}$). The pore size is mainly less than 20 nm (inset in Figure 2a), consistent with the TEM observation (Figure 1h and its inset). Such a 10-fold increase in the specific surface area of g-C_3N_4 (550) "seaweed" should be beneficial for its application as a photocatalyst as a more exposed interfacial contact to the reactant would be highly demanded.

For X-ray diffraction (XRD) analysis, g-C_3N_4 bulk features two peaks (Figure 2b) at 13.3° and 27.4° arising from an in-plane structural packing motif and an interlayer stacking reflection of conjugated aromatic segments, respectively.[4d,5–7] Compared to g-C_3N_4 bulk, g-C_3N_4 (550) "seaweed" shows a shift and widened diffraction peak appears at about 26.8°, indicating a slightly enlarged interlayer spacing.[4,7] The peak located at 13.3° was absent for g-C_3N_4 (550) "seaweed", suggesting a smaller planar size,[4,7] as observed in TEM image (Figure 1h). As g-C_3N_4 (550) "seaweed" has a mesoporous structure and exhibits much smaller and thinner particles/sheets than g-C_3N_4 bulk (Figure S2), it can be homogenously dispersed in water with concentrations of 1 mg mL^{-1} without precipitation even after storage for two weeks under ambient conditions, in sharp contrast to the poor dispersibility observed for g-C_3N_4 bulk (Figure S3), which thus favors a maximized exposure of catalytic species to water. FT-IR spectrum of g-C_3N_4 (550) "seaweed" exhibits several strong bands in the region 1200–1700 cm^{-1} (Figure 2c), which belong to the typical stretching modes of CN heterocycles. The peak at approximately 810 cm^{-1} originates from the characteristic breathing mode of tri-s-triazine units.[4d,5–7] There is an enhanced absorption for g-C_3N_4 "seaweed" in the 2900–3600 cm^{-1} range corresponding to the surface-bonded H_2O molecules and amino groups, which indicate the enlarged open-up surfaces.[7] X-ray photoelectron spectroscopy (XPS) shows g-C_3N_4 "seaweed" has a similar chemical composition to that of g-C_3N_4 bulk (Figure S4a). High resolution N1s spectrum of g-C_3N_4 (550) "seaweed" (Figure 2d) reveals the existence of sp^2-hybridized nitrogen (N1) at 398.8 eV, the tertiary nitrogen ($N(C)_3$, N2) at 399.7 eV and the amino functional groups (N3) at 400.8 eV.[4–7] Accordingly, C1s spectrum (Figure S4b) shows the C–C, N-C=N, and C–O bands,[4–7] which match with the energy dispersive X-ray (EDX) spectrum (Figure S5). Overall, g-

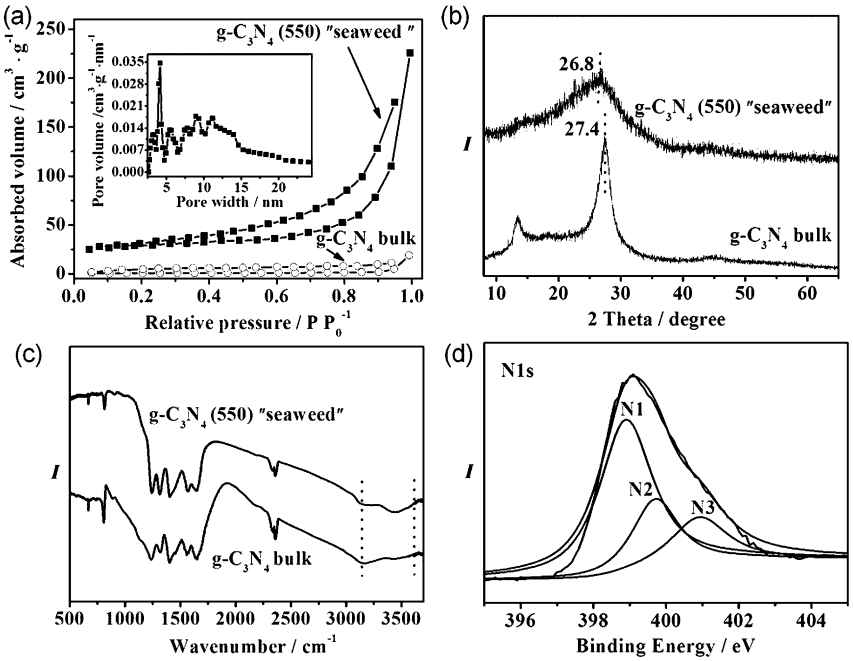

Figure 2. a) N_2 adsorption isotherms of g-C_3N_4 (550) "seaweed" and g-C_3N_4 bulk. Inset: pore size distribution of g-C_3N_4 (550) "seaweed"; b) XRD patterns and c) FT-IR spectrum of g-C_3N_4 (550) "seaweed" and g-C_3N_4 bulk; d) The high-resolution N1s XPS spectrum of g-C_3N_4 (550) "seaweed".

C_3N_4 (550) "seaweed" has the intrinsic structure of typical g-C_3N_4 but with a hierarchical nanostructured high surface area that could potentially lead to a largely improved evolution rate of water splitting.

The hierarchical nanostructured architectures greatly altered the optical properties of g-C_3N_4(550) "seaweed" compared to g-C_3N_4 bulk. In Figure 3a, the photoabsorption

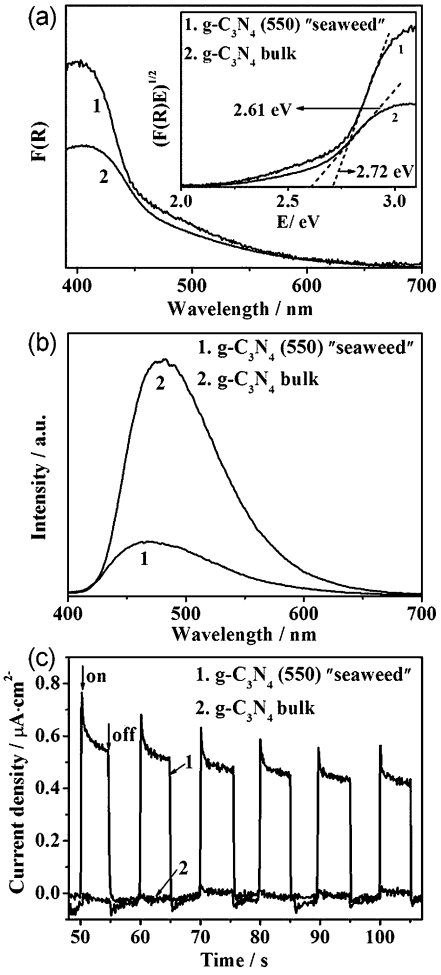

Figure 3. a) UV/Vis diffuse reflectance spectra of 1) g-C_3N_4(550) "seaweed" and 2) g-C_3N_4 bulk (Inset: bandgap energies); b) PL spectra of 1) g-C_3N_4(550) "seaweed" and 2) g-C_3N_4 bulk with the excitation wavelength of 400 nm; c) Transient photocurrents under visible light illumination ($\lambda > 420$ nm) of 1) g-C_3N_4(550) "seaweed" and 2) g-C_3N_4 bulk obtained at 0.1 V vs. Ag/AgCl in a 0.2 M Na_2SO_4 aqueous solution pH 6.8).

edge of g-C_3N_4(550) "seaweed" displays a hypochromic shift from 475 nm to 455 nm. The corresponding bandgap energy increases from 2.61 eV to 2.72 eV, indicating the quantum confinement effect in g-C_3N_4(550) "seaweed" (Figure 3a inset).[4d,e] Furthermore, a remarkably enhanced light-harvesting ability is also discovered for g-C_3N_4(550) "seaweed" across the whole optical spectrum, mainly arising from multiple scattering effects and the existence of large numbers of defect sites associated with the mesoporous surfaces.[7,10a] The structure-induced property change can also be observed in the photoluminescence spectra. As shown in Figure 3b and Figure S6, the otherwise strong photoluminescence is quenched, suggesting that the energy-wasteful charge recombination is substantially suppressed, and thus improving charge separation.[10a,b] The property change should be attributed to the structural benefits of g-C_3N_4(550) "seaweed" because its open-framework construction can create new surface states for charge traps. Furthermore, and g-C_3N_4(550) "seaweed" featuring 1D thin fibers might facilitate photogenerated electron transfer onto its surfaces for reacting with water molecules, which could in return inhibit the charge recombination. The clear enhancement of photocurrent (Figure 3c) for g-C_3N_4(550) "seaweed" indicates an improved charge separation, and therefore an enhancement of the photocatalytic performance.[5,6]

The photocatalytic activities of g-C_3N_4(550) "seaweed" was examined for hydrogen evolution from water by using 3 wt% Pt as a co-catalyst and 10 vol% triethanolamine as an electron donor under visible light irradiation ($\lambda > 420$ nm). As shown in Figure 4a, 1.2 mmol H_2 gas (26.9 mL) was produced

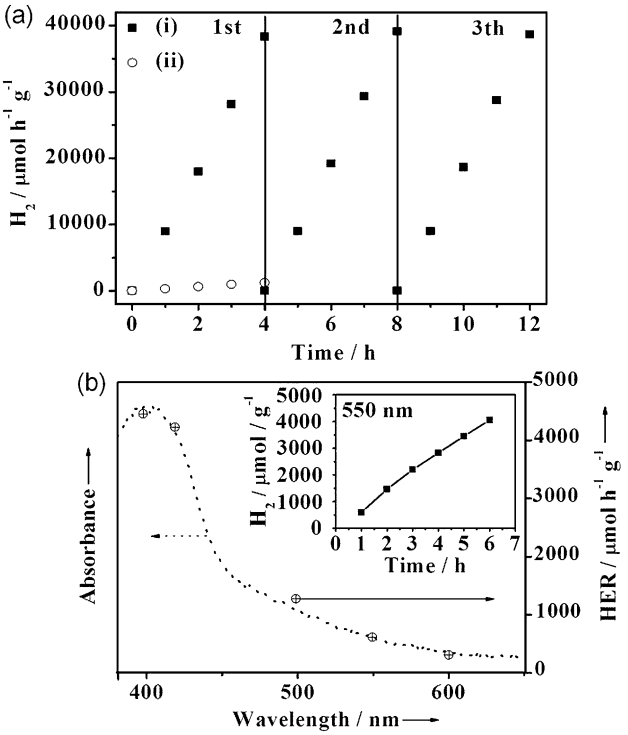

Figure 4. a) Photocatalytic activities of g-C_3N_4 (550) "seaweed" (i) and g-C_3N_4 bulk (ii) under irradiation with visible light ($\lambda > 420$); b) Wavelength dependence of H_2 evolution rate on g-C_3N_4(550) "seaweed" (inset: the H_2 evolution under 550 nm light irradiation).

without noticeable deactivation after 12 h. The hydrogen evolution rate (HER) of g-C_3N_4(550) "seaweed" steadily reaches to 9900 $\mu mol\,h^{-1}\,g^{-1}$, over thirty times that of g-C_3N_4 bulk (300 $\mu mol\,h^{-1}\,g^{-1}$). In addition it has a turnover number (TON) of 385 in 6 h, much higher than that of g-C_3N_4 bulk (2.3) (Figure S7). Wavelength dependence of H_2 evolution reveals the activity of g-C_3N_4(550) "seaweed" corresponds to its optical absorption spectrum, suggesting that the H_2

production is primarily driven by photo-induced electrons in carbon nitride polymer (Figure 4b).[7] The calculated apparent quantum efficiency of g-C_3N_4(550) "seaweed" is 7.8% under irradiation at 420 nm. In addition, g-C_3N_4(550) "seaweed" still shows a nearly linear profile of photocatalytic activity (HER = 614 μmol h^{-1} g^{-1}) for 6 h at 550 nm monochromic illumination (Figure 4b inset).

For comparison, a series of g-C_3N_4 "seaweed" samples were obtained by calcining the precursors of the freeze-drying assembled HTD under controlled temperatures. The g-C_3N_4 "seaweed" samples obtained by calcination at 500 °C, 600 °C, and 650 °C were designated as g-C_3N_4(500), (600), and (650) "seaweed", respectively. All the g-C_3N_4 "seaweed" samples are mesoporous fiber networks (Figure S8) and show similar XRD patterns and IR spectra (Figure S9 and S10) to g-C_3N_4 (550) "seaweed". BET surface areas of g-C_3N_4 (500), (600), and (650) "seaweed" are around 103 cm^2 g^{-1}, 135 cm^2 g^{-1} and 147 cm^2 g^{-1}, respectively, closely to that of g-C_3N_4(550) "seaweed" and much larger than that of g-C_3N_4 bulk. Note that the HER of g-C_3N_4(550) "seaweed" is the highest versus other samples (Figure 5a). This performance variation may be directly associated with the effect of the nitrogen species according to previous reports.[11] As shown in Figure S11 and Table S1, the ratio of sp^2 C–N=C bonds to the sum of sp^3 N–$[C]_3$ and C–NH_x bonds for g-C_3N_4(550) "seaweed" was 1.48, higher than those samples treated at 500 °C, 600 °C, and 650 °C (1.24, 1.30, and 1.27, respectively), indicating that the sp^2-bonded nitrogen atom contributes more to the bandgap absorption than other nitrogen species,[11] thus inducing a larger enhancement in photocatalytic activity. The optimal g-C_3N_4(550) "seaweed" with the excellent HER of 9900 μmol h^{-1} g^{-1} and apparent quantum efficiency of 7.8% at 420 nm is greater than most of the nanostructured g-C_3N_4 photocatalysts reported (Figure 5b and Table S2), except g-C_3N_4 nanospheres.[7] However, for the preparation of g-C_3N_4 nanospheres, silica spheres were usually used as sacrificial templates, a large amount of organic solvents (e.g., tetraethyl orthosilicate, cyclohexane, cetylpyridinium bromide), and a tedious multistep process were involved, that is challenging to scale up into large quantity production.

In summary, we have successfully assembled 1D nanofibers of g-C_3N_4 with mesoporous structure into a "seaweed" architecture by using a simple method of freeze-drying self-assembly approach. The product has improved electron-transfer ability, enhanced light harvesting, and increased active sites, it exhibits highly efficient photocatalytic activity, better than most nanostructured g-C_3N_4 catalysts. This work provides a simple method for large-scale constructing the new type of g-C_3N_4 nanostructured materials for a large variety of optoelectronic devices and biological applications.

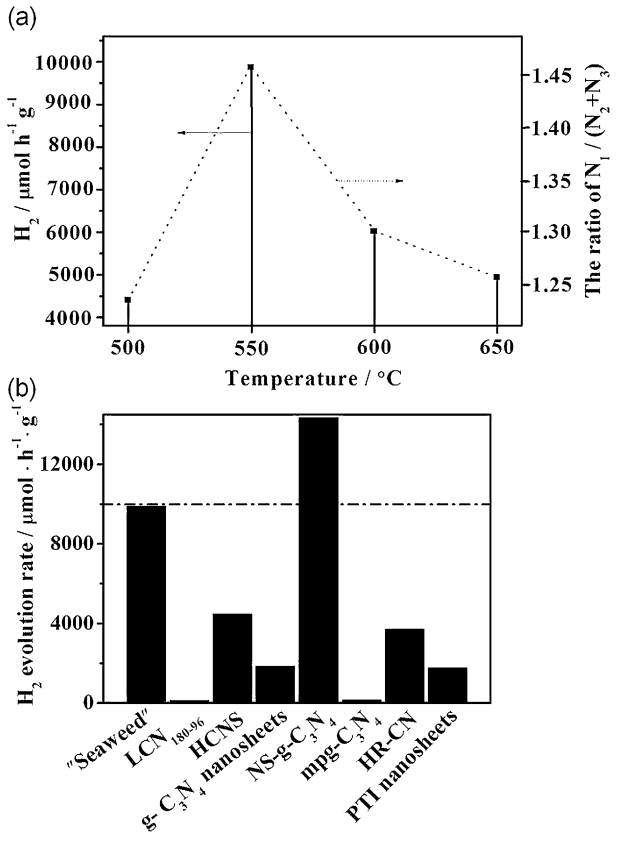

Figure 5. a) Hydrogen-evolution rate of g-C_3N_4(500), (550), (600), and (650) "seaweed" samples prepared at the indicated temperatures (dotted line is to guide the eye); b) The Hydrogen-evolution rate for various nanostructured g-C_3N_4 photocatalysts ("seaweed" representing g-C_3N_4(550) "seaweed" in this work, $LCN_{180\text{-}96}$ Ref. [5]. HCNS Ref. [8b], g-C_3N_4 nanosheets Ref. [6a], NS-G-C_3N_4 Ref. [7], mpg-C_3N_4 Ref. [10a], HR-CN Ref. [8c], PTI-nanosheets Ref. [8d]).

Experimental Section

Synthesis: Dicyandiamide (0.50 g) was added into deionized water (12.5 mL), and the mixture was placed into a sonic bath for 30 min to obtain a homogeneous solution. The solution was sealed in a Teflon-lined autoclave at 200 °C for 4 h, and then kept in liquid nitrogen to induce the freezing assisted assembly. The final sample was collected by thermal treatment of the freeze-dried HTD at different temperatures (500 °C to 650 °C) with a ramp rate of 1 °C min^{-1} in Ar flow. The hydrothermal pretreatment prior to the vacuum freeze-drying process has a significant effect on the morphology and performance of the final g-C_3N_4 "seaweed" products, which has been discussed in detail in Figure S12–S17 in Supporting Information). For comparison, the g-C_3N_4 bulk was synthesized by directly heating dicyandiamide from room temperature to 550 °C in Ar with a ramp rate of 1 °C min^{-1} and stabilized for 4 h, then cooled to room temperature.

Characterization: The morphology of the samples was investigated by scanning (SEM, JSM-7500) and transmission (TEM, 7650B, Hitachi) electron microscopy. XRD patterns were obtained by using a Netherlands 1,710 diffractometer with a Cu K_α irradiation source (λ = 1.54 Å). FTIR spectra were recorded on a Bruker spectrometer (Equinox 55/S) using KBr pellets. XPS data were obtained with an ESCALab220i-XL electron spectrometer from VG Scientific using 300 W Al K_α radiation. The UV/Vis absorption and the photoluminescence spectra were measured with a 5300pc spectrophotometer and a SPEX flourolog-3 fluorimeter. BET specific surface area was determined by nitrogen adsorption–desorption isotherm measurements at 77 K (NOVA 2200e).

Photocatalytic tests: Photocatalytic water splitting was carried out in a top-irradiation vessel connected to a gas-closed glass system. Photocatalyst powder (10 mg) was dispersed in aqueous solution (100 mL) containing 10 vol% triethanolamine scavenger and 3 wt% (respect to Pt, acting as co-catalysts) $H_2PtCl_6 \cdot 6H_2O$. The temperature of the reaction solution was carefully maintained below 6 °C during the whole experiment. The reactor was then sealed and evacuated

several times to remove air before irradiated under a 300 W Xe lamp equipped with a 420 nm cutoff filter. The amount of evolved H_2 was analyzed by gas chromatography (GC-7920) with high-purity nitrogen carrier gas.

Keywords: g-C_3N_4 "seaweed" · hydrogen evolution · photocatalysis · self-assembly · template-free

How to cite: *Angew. Chem. Int. Ed.* **2015**, *54*, 11433–11437
Angew. Chem. **2015**, *127*, 11595–11599

[1] K. Maeda, K. Teramura, D. L. Lu, T. Takata, N. Saito, Y. Ioune, K. Domen, *Nature* **2006**, *440*, 295.
[2] X. B. Chen, S. H. Shen, L. J. Guo, S. S. Mao, *Chem. Rev.* **2010**, *110*, 6503–6570.
[3] X. C. Wang, K. Maeda, A. Thomas, K. Takanabe, G. Xin, J. M. Carlsson, K. Domen, M. Antonietti, *Nat. Mater.* **2008**, *8*, 76–80.
[4] a) X. Wang, X. Chen, A. Thomas, X. Fu, M. Antonietti, *Adv. Mater.* **2009**, *21*, 1609–1612; b) G. Liu, P. Niu, C. H. Sun, S. C. Smith, Z. G. Chen, G. Q. Lu, H. M. Cheng, *J. Am. Chem. Soc.* **2010**, *132*, 11642–11648; c) Z. Z. Lin, X. C. Wang, *Angew. Chem. Int. Ed.* **2013**, *52*, 1735–1738; *Angew. Chem.* **2013**, *125*, 1779–1782; d) G. G. Zhang, M. W. Zhang, X. X. Ye, X. Q. Qiu, S. Lin, X. C. Wang, *Adv. Mater.* **2014**, *26*, 805–809; e) Q. Han, C. G. Hu, F. Zhao, Z. P. Zhang, N. Chen, L. T. Qu, *J. Mater. Chem. A* **2015**, *3*, 4612–4619.
[5] Y. J. Cui, Z. X. Ding, X. Z. Fu, X. C. Wang, *Angew. Chem. Int. Ed.* **2012**, *51*, 11814–11818; *Angew. Chem.* **2012**, *124*, 11984–11988.
[6] a) S. B. Yang, Y. J. Gong, J. S. Zhang, L. Zhan, L. L. Ma, Z. Y. Fang, R. Vajtai, X. C. Wang, P. M. Ajayan, *Adv. Mater.* **2013**, *25*, 2452–2457; b) Q. Han, F. Zhao, C. G. Hu, L. X. Lv, Z. P. Zhang, N. Chen, L. T. Qu, *Nano Res.* **2015**, *8*, 1718–1728.
[7] J. S. Zhang, M. W. Zhang, C. Yang, X. C. Wang, *Adv. Mater.* **2014**, *26*, 4121–4126.
[8] a) Y. S. Jun, J. Park, S. U. Lee, A. Thomas, W. Hi, G. D. Stucky, *Angew. Chem. Int. Ed.* **2013**, *52*, 11083–11087; *Angew. Chem.* **2013**, *125*, 11289–11293; b) J. H. Sun, J. S. Zhang, M. W. Zhang, M. Antonietti, X. Z. Fu, X. C. Wang, *Nat. Commun.* **2012**, 1139; c) Y. Zheng, L. H. Lin, X. J. Ye, F. S. Guo, X. C. Wang, *Angew. Chem. Int. Ed.* **2014**, *53*, 11926–11930; *Angew. Chem.* **2014**, *126*, 12120–12124; d) K. Schwinghammer, M. B. Mesch, V. Duppel, C. Ziegler, J. Senker, B. V. Lotsch, *J. Am. Chem. Soc.* **2014**, *136*, 1730–1733.
[9] a) V. N. Khabashesku, J. L. Zimmerman, J. L. Margrave, *Chem. Mater.* **2000**, *12*, 3264–3270; b) J. L. Zimmerman, R. Williams, V. N. Khabashesku, J. L. Margrave, *Nano Lett.* **2001**, *1*, 731–734.
[10] a) X. Wang, K. Maeda, X. Chen, K. Takanabe, K. Domen, Y. Hou, X. Fu, M. Antonietti, *J. Am. Chem. Soc.* **2009**, *131*, 1680–1681; b) K. Kailasam, J. D. Epping, A. Thomas, S. Losse, H. Junge, *Energy Environ. Sci.* **2011**, *4*, 4668–4674.
[11] D. J. Martin, K. P. Qiu, S. A. Shevlin, A. D. Handoko, X. W. Chen, Z. X. Guo, J. W. Tang, *Angew. Chem. Int. Ed.* **2014**, *53*, 9240–9245; *Angew. Chem.* **2014**, *126*, 9394–9399.

Received: June 2, 2015
Published online: July 14, 2015

